Mon. Not. R. Astron. Soc. **364,** L13–L17 (2005) doi:10.1111/j.1745-3933.2005.00095.x

A radial velocity survey of low Galactic latitude structures – II. The Monoceros Ring behind the Canis Major dwarf galaxy

Blair C. Conn,[1⋆] Nicolas F. Martin,[2,3⋆] Geraint F. Lewis,[1⋆] Rodrigo A. Ibata,[2⋆] Michele Bellazzini[4⋆] and Mike J. Irwin[3⋆]

[1]*Institute of Astronomy, School of Physics, A29, University of Sydney, NSW 2006, Australia*
[2]*Observatoire de Strabourg, 11, rue de l'Université, F-67000, Strasbourg, France*
[3]*Institute of Astronomy, Madingley Road, Cambridge CB3 0HA*
[4]*INAF – Osservatorio Astronomico di Bologna, Via Ranzani 1, 40127, Bologna, Italy*

Accepted 2005 August 17. Received 2005 August 9; in original form 2005 July 4

ABSTRACT

An AAT/2dF Spectrograph Survey of low Galactic latitudes targeting the putative Canis Major dwarf galaxy and the (possibly) associated tidal debris of stars known as the Monoceros Ring, covering Galactic coordinates $231\overset{\circ}{.}5 < l < 247\overset{\circ}{.}5$ and $-11\overset{\circ}{.}8 < b < -3\overset{\circ}{.}8$, has revealed the presence of the Monoceros Ring in the background of the Canis Major dwarf galaxy. This detection resides at a Galactocentric distance of $\sim 18.9 \pm 0.3$ kpc (13.5 ± 0.3 kpc heliocentric), exhibiting a velocity of $\sim 132.8 \pm 1.3\,\mathrm{km\,s^{-1}}$ with a dispersion of $\sim 22.7 \pm 1.7\,\mathrm{km\,s^{-1}}$, both of these comparable to previous measurements of the Monoceros Ring in nearby fields. This detection highlights the increasing complexity of structure being revealed in recent surveys of the Milky Way thick disc and halo.

Key words: Galaxy: structure – Galaxy: formation – galaxies: interactions.

1 INTRODUCTION

Galaxy formation based on a Λ cold dark matter (ΛCDM) cosmology predicts larger structures being formed from the accumulation of smaller systems (e.g. Searle & Zinn 1978; White & Rees 1978; White 1978; Abadi et al. 2003b,a). One of the core outcomes of this model is that the haloes of galaxies should be strewn with the debris from all these minor mergers. The first discovery of such a merger within our own Milky Way, the Sagittarius dwarf galaxy (Ibata, Gilmore & Irwin 1994), demonstrated that such mergers do occur and are in fact ongoing.

Insight into the complex nature of the Galactic halo has been in part accomplished by recent all-sky surveys, the Sloan Digital Sky Survey (SDSS) and the Two Micron All Sky Survey (2MASS). Investigating an overdensity of F-turn-off stars in the SDSS, Newberg et al. (2002) discovered the presence of a stream of stars suggestive of an equatorial accretion event around the Milky Way. Unlike the Sagittarius dwarf galaxy which is on a polar orbit, this accretion event may have implications for the formation of key Galactic structures, such as the thick disc. The equatorial orbit of the stream was investigated by Crane et al. (2003) who targeted 2MASS-selected M-giant stars in the range $l = 150^\circ$–240°, although primarily in the Northern hemisphere, finding that a simple circular orbit model with a Galactocentric radius of 18 kpc and a velocity of $\sim 220\,\mathrm{km\,s^{-1}}$ best fitted the data. The velocity dispersion of their sample was $20 \pm 4\,\mathrm{km\,s^{-1}}$ which excludes it from being of Galactic origins. As more detections of this structure were made (Ibata et al. 2003; Rocha-Pinto et al. 2003; Yanny et al. 2004) it became clear that, as proposed by Newberg et al. (2002), this was indeed another on-going accretion event. The search for the progenitor of the stream in the 2MASS catalogue led Martin et al. (2004a) to uncover the Canis Major dwarf galaxy, $(l, b) = \sim(240^\circ, -8^\circ)$.

Because of the low density of stream material on the sky, it has been necessary to employ the use of wide-field cameras to look deeply into the thick disc and halo of the Milky Way, not only confirming and enhancing previous detections, but also probing new regions, leading to more detections of the Monoceros Ring and the Canis Major dwarf being made (Martin et al. 2004a; Bellazzini et al. 2004; Conn et al. 2005; Martínez-Delgado et al. 2005). Detections of an additional structure in Triangulum–Andromeda (Rocha-Pinto et al. 2004; Majewski et al. 2004) are revealing the increasing complexity of accretion events in the outer regions of the Galaxy. Current debate on these detections centres on whether these represent separate accretion events or are the product of a single ongoing merger. The location of the progenitor is still contentious, but this paper will refer to the Canis Major overdensity as the Canis Major dwarf galaxy (CMa), following the conclusions of Martínez-Delgado et al. (2005) and Martin et al. (2005a).

While the positions of the streams on the sky are highly accurate, the distance estimates to the stars are less so, requiring the need for radial velocity kinematic measurements to increase and

⋆E-mail: bconn@physics.usyd.edu.au (BCC); martin@astro.u-strasbg.fr (NFM); gfl@physics.usyd.edu.au (GFL); ibata@astro.u-strasbg.fr (RAI); michele.bellazzini@bo.astro.it (MB); mike@ast.cam.ac.uk (MJI)

characterize the known properties of the streams. Distances are then estimated through photometric parallaxes as described by Martin et al. (2004b). To date, several kinematic surveys of the Monoceros Stream have been undertaken using the data of 2MASS and SDSS (Crane et al. 2003; Yanny et al. 2004; Rocha-Pinto et al. 2004). These have confirmed a velocity gradient with Galactic longitude and also a low velocity dispersion of $\sigma_{(v_r)} \sim 20$ km s^{-1} for the Monoceros Ring.

While most models of equatorial accretion on to disc-like galaxies (e.g. Peñarrubia et al. 2005; Martin et al. 2005a) predict the presence of multiply wrapped streams, no detections provide conclusive evidence supporting this hypothesis. This is most likely due to the pencil-beam nature of most fields with regard to the entire structure on the sky, and given that confirmed detections of the stream are limited to Galactic longitudes $120^\circ < l < 240^\circ$ and significant areas of this structure are yet to be sampled. This new detection presented here is consistent with multiply wrapped streams.

2 OBSERVATIONS AND REDUCTION

In 2004 April, a survey was undertaken with the Two-degree Field (2dF) multi-fibre spectrograph on the Anglo-Australian Telescope (AAT) with two aims: first to determine the kinematics of the Canis Major dwarf; and secondly to try to locate the stars belonging to the Monoceros Ring through kinematic constraints. Out of ∼15 fields, eight were dedicated to this purpose, four focusing solely on the Canis Major region. This paper will focus primarily on results pertaining to the detection of the Monoceros Ring in the Canis Major dwarf region, the same area as studied by Martin et al. (2005a, hereafter Paper I).

The 2dF instrument is capable of measuring velocities of ∼400 stars simultaneously within a 2° field of view. The field is divided between two spectrographs, the first using a 1200V grating (4600–5600 Å at 1 Å pixel^{-1}); the second using a 1200R grating (8000–9000 Å at 1 Å pixel^{-1}). The configuration on the second spectrograph was chosen to target red clump stars in the distance range 5–8 kpc; these stars fall outside the distance range expected for the Monoceros Ring and thus are not discussed in this paper. (Paper I discusses the results of the survey in the region <10 kpc.)

The red giant branch (RGB) stars in this survey were chosen from Sample A of Martin et al. (2004a). Using the photometric parallax technique of Majewski et al. (2003) to determine the distances, the stars in the correct distance range for the Monoceros Ring can then be easily selected. Determining the exact error on the distance using this technique is difficult, and so for these observations a conservative estimate of ±1 kpc for these stars has been assumed. The J, H and K magnitudes from the 2MASS catalogue for these stars have been de-reddened using the dust maps of Schlegel, Finkbeiner & Davis (1998) and the asymptotic correction of Bonifacio, Monai & Beers (2000).

2.1 Reducing 2dF spectra

Data reduction of the 2dF spectra involves using the 2DFDR package (Taylor et al. 1996) which applies the flat-field correction and sky subtraction, and extracts the individual spectra from each fibre off the CCD. Because of an asymmetry in the line spread function (LSF) of the spectra, a *custom-made* reduction pipeline was constructed to minimize the errors that this produced when comparing with radial velocity standard stars; a detailed presentation of the pipeline can be found in Martin et al. (2005b). This pipeline limits the systematic offsets in the radial velocity due to the LSF to ±5 km s^{-1}; this value is not included in the errors stated. Determining the radial velocities, v_r, using several artificial standard star templates and taking a weighted average of the solutions avoids any systematic offset that may result from a peculiarity in one of the templates (Paper I; Martin et al. 2005b). Stars with $\sigma_v > 5$ km s^{-1} (see equation 2 of Paper I) are removed from the sample to avoid contaminating the results with poor determination of radial velocity. Dust extinction in this region typically is $E(B-V) < 0.4$ (taken from Schlegel et al. 1998) and only the field closest to the plane has higher extinction. There has been no significant impact on the 2MASS colours due to extinction.

2.2 Determining the fit and the associated error

For each velocity and distance distribution, a Gaussian has been fitted to the profile using an AMOEBA routine (Press et al. 1992), obtaining a characteristic velocity, velocity dispersion, distance and distance dispersion that best represent the data. The errors on the fitted parameters have been determined by bootstrap re-sampling and then refitting the data. The re-sampling was undertaken using the errors of each quantity, namely the conservative ±1 kpc for the distance to each star and the root-mean-square value of the dispersion. The errors cited, then, are the standard deviations of the fit determined using this method. There is no appreciable difference between the Galactocentric and heliocentric errors in this field. The velocity errors also have an additional ±5 km s^{-1} systematic error on top of the stated errors.

3 RESULTS

3.1 The Monoceros Ring behind the Canis Major dwarf

The data in Fig. 1 were taken from six fields of the 2dF spectrographic survey and show a population of ∼38 RGB stars behind the Canis Major overdensity. These stars are represented in the solid histogram, while the dotted histogram shows the remaining stars in that region. The stars have been selected using the following criteria: $231.^\circ5 < l < 247.^\circ5$ and $-11.^\circ8 < b < -3.^\circ8$; $12 < D_\odot < 20$ kpc and a colour cut of $0.9 < (J-K)_0 < 1.3$, $0.561(J-K)_0 + 0.22 < (J-H)_0 < 0.561(J-K)_0 + 0.36$ and $K_0 \leqslant 13.0$; with $v_r > 0$ km s^{-1}. This overdensity shows up very clearly in the Galactocentric distance histogram, and given the distance range of these stars, makes them different from the foreground Canis Major stars as presented in Paper I. They form a coherent velocity and distance structure similar to that of previous Monoceros Ring detections. Fig. 1 shows the 2dF data with a Gaussian fit of $v_r = 132.8 \pm 1.3$ km s^{-1} and an internal dispersion of 22.7 ± 1.7 km s^{-1}, which is comparable to the dispersion as measured by Yanny et al. (2004) from SDSS data. The Galactocentric distance estimates to this feature are 18.9 ± 0.3 kpc with a dispersion of 0.8 ± 0.4 kpc. See Section 2.2 or Paper I for a more complete breakdown of the errors; however, note again that the errors have an additional systematic offset of ±5 km s^{-1}. To test the contamination of local dwarfs that fall inside the selection criteria for the sample stars because of poor extinction correction, the data have been tested with a more stringent cut-off of $(J-K)_0 > 0.95$. This still reproduces the detection presented here, suggesting that the contamination level is low.

Although, as can be seen in Fig. 1, there is no definitive evidence for a *gap* between the Canis Major detection and the Monoceros Ring detection, this is most likely due to the large errors in the distance rather than the structure being somewhat continuous out to large Galactocentric distances. The conservatively estimated error

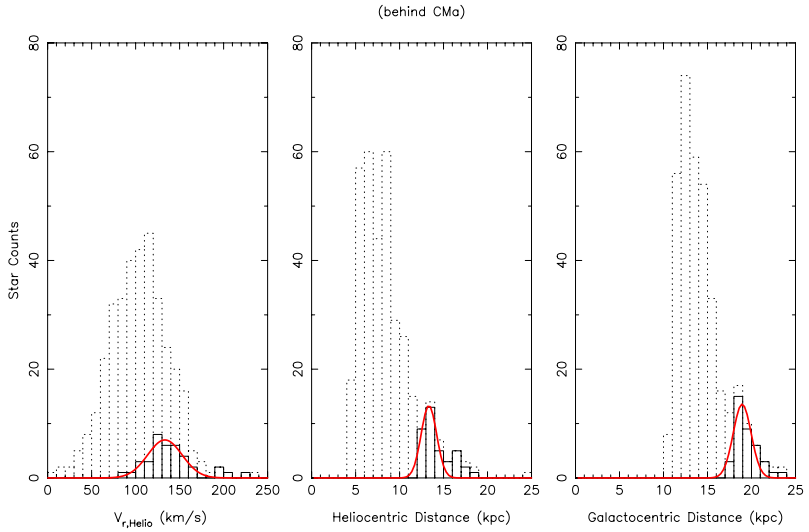

Figure 1. Histograms of the 2dF RGB data in the range $231.^\circ5 < l < 247.^\circ5$ and $-11.^\circ8 < b < -3.^\circ8$, with a heliocentric distance cut of $12 < D_\odot < 20$ kpc and the following additional cuts of $0.9 < (J-K)_0 < 1.3$, $0.561(J-K)_0 + 0.22 < (J-H)_0 < 0.561(J-K)_0 + 0.36$, $K_0 \leqslant 13.0$ and $v_r > 0\,\mathrm{km\,s^{-1}}$. This field constitutes the region behind the Canis Major overdensity, revealing a detection of the Monoceros Ring at a Galactocentric distance of 18.9 ± 0.3 kpc and a dispersion of 0.8 ± 0.4 kpc (right-hand panel), with a heliocentric distance of 13.5 ± 0.3 kpc with similar dispersion (middle panel). The velocity profile fitted to this population is $v_r = 132.8 \pm 1.3\,\mathrm{km\,s^{-1}}$ with an internal dispersion of $22.7 \pm 1.7\,\mathrm{km\,s^{-1}}$ (left-hand panel); the error is accompanied by an additional systematic offset of $\pm 5\,\mathrm{km\,s^{-1}}$. The dotted lines shows the remaining data outside the distance and colour cuts. For a full outline of the errors, see Section 2.2 and Paper I.

on the distance is ∼1 kpc, which will have the effect of blurring any intrinsic gap between the two structures. Contamination from local dwarfs, although believed to be minimal, will also impact on the ability to resolve the stream out cleanly from the Canis Major population. It should also be noted that, depending on the formation scenario of the stream, the stars may or may not be neatly confined at one distance but rather diffused over a larger volume. Since the origins and evolution of both structures are still being investigated, explaining the lack of a gap in distance is at best speculative. With these stars being selected from the 2MASS catalogue, a measure of the completeness of the sample becomes possible. Applying the colour cuts used on the 2dF data to the 2MASS catalogue reveals 399 stars in this region of which 364 have been observed, making this sample ∼91 per cent complete.

In Paper I, a northern comparison field at $(240.^\circ0, +8.^\circ8)$ is presented for the Canis Major detection. Unfortunately, the number of RGB stars sampled out to large Galactic radii is too low to form a useful comparison with the detection presented in this paper.

3.2 The Besançon synthetic galaxy model

Understanding what the Galactic contribution is in any given region of sky is critical when attempting to interpret the results of this 2dF survey. To investigate this, the synthetic galaxy model of Robin et al. (2003) is used to find out what the model predicts that our Galactic contamination should be. This is done by selecting exactly the same regions of sky as observed in the 2dF survey. Given the tight constraints in colour and magnitude used to select the stars in our survey (see Paper I), applying the same constraints to the synthetic Galaxy model to provide an idea of the contamination that we should expect was undertaken. In particular, these constraints are $0.9 < (J-K)_0 < 1.3$, $0.561(J-K)_0 + 0.22 < (J-H)_0 < 0.561(J-K)_0 + 0.36$, $K_0 \leqslant 13.0$, and $v_r > 0\,\mathrm{km\,s^{-1}}$. The cuts were applied to the model which extended to a heliocentric distance of 100 kpc.

To remove the presence of noise in the model, each field was investigated using the online model, selecting the 'small field' setting with a solid angle of 1000 deg^2. This has the effect of providing a smoother distribution of the stars with the properties determined by the centre of the field, rather than the 'large field' option which takes into account changes in (l, b). Each field was then rescaled back to the size of the 2dF fields and rescaled to match the completeness of the 2dF sample with regard to the 2MASS catalogue. These stars are presented in Fig. 2, and in general have a much broader distribution than could be attributed to any tidal debris, with velocities that typically peak well away from the 2dF detections. As expected, in the distance range of the Monoceros Ring there is no thin disc population, and the thick disc has only ∼15 stars in this location; halo stars are expected to have only a very small presence in this field and are not included in these results. The comparisons with the Besançon model provide good support for the validity of this detection with the usual precautions.

The approximately 15 stars that fall in the region of the Monoceros Ring in the model have the following properties: a velocity profile of $v_r = 143.8\,\mathrm{km\,s^{-1}}$ and a dispersion of $28.2\,\mathrm{km\,s^{-1}}$; and a Galactocentric distance of 19.7 kpc with a dispersion of 1.9 kpc. A Kolmogorov–Smirnov test of the Monoceros Ring stars from the 2dF sample and the Besançon stars finds a 4 per cent chance of the two being drawn from the same distribution. This is a relatively high probability of coincidence; however, a few extra factors need to be taken into account. While the model contains thick disc stars with an additional warp component, the data contain thick disc stars, CMa stars and Monoceros Ring stars with a warp component mixed in. What effect does this have on our comparison? Since a completeness factor has been derived from the 2MASS catalogue and subsequently used to scale the Besançon model, and given that the 2MASS stars contain a significant proportion of CMa stars, then the numbers of thick disc stars must be being overestimated. This has the immediate effect of lowering the number of stars that can be expected in the distance range of the Monoceros Ring. The true number of Galactic

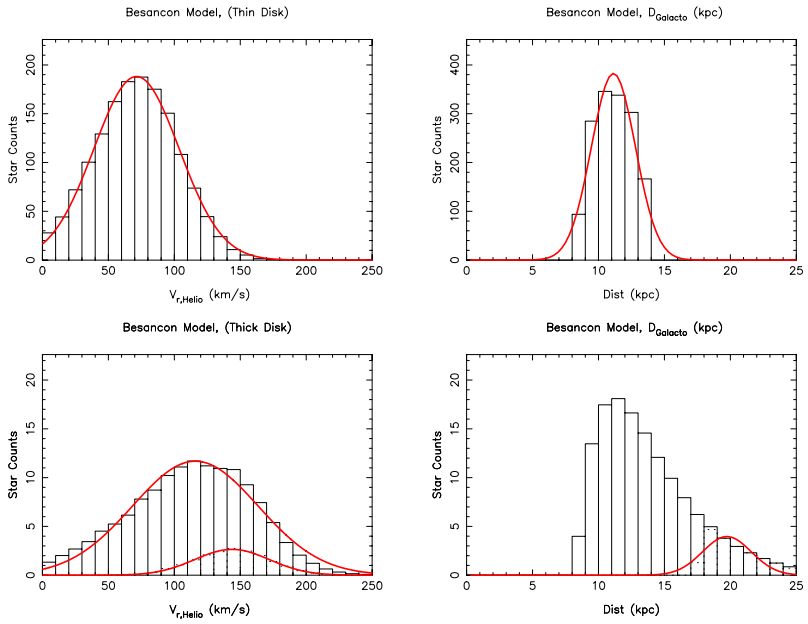

Figure 2. Histograms of Besançon data covering the same region of sky as the 2dF data set; no distance cuts have been applied less than the 100-kpc cut-off of the model. The distances are Galactocentric to allow easy comparison with the 2dF data as shown in Fig. 1. The top panels show the thin disc population (stars in the age range 5–7 Gyr) in this field fitted with a Gaussian profile at a distance of ∼11.1 kpc and a dispersion of ∼1.7 kpc. The velocity profile of the thin disc stars is $v_r = \sim 71.4\,\mathrm{km\,s^{-1}}$ with a dispersion of $\sim 32.3\,\mathrm{km\,s^{-1}}$. In the bottom panels are the thick disc stars (noting that these stars have a different density profile from the thin disc stars): they too can be fitted with a Gaussian profile and reside at a Galactocentric distance of 13.1 kpc with a dispersion of 5.0 kpc; the velocity and dispersion are found to be $v_r = 115.9$ and $47.7\,\mathrm{km\,s^{-1}}$ respectively. The smaller Gaussians represent those 15 stars in the same distance range as the Monoceros Ring stars in Fig. 1 with $v_r = 143.8\,\mathrm{km\,s^{-1}}$ and a dispersion of $28.2\,\mathrm{km\,s^{-1}}$, and a Galactocentric distance of 19.7 kpc with a dispersion of 1.9 kpc.

thick disc stars would be much less than the ∼15 stars presented in Fig. 2, especially since most of the stars as presented in Paper I seem to belong to the CMa structure, and since confusion over whether they represent the warp seems to have been sufficiently discounted.

4 DISCUSSION AND CONCLUSION

Comparisons with the Besançon synthetic galaxy model (Fig. 2) reveal that the peak velocity and dispersion observed in this field cannot be associated with any known Galactic component. The thick disc component in the same region as the Monoceros Ring has a higher velocity and a broader velocity dispersion, which discount it as the cause of the overdensity measured in this field (see Fig. 1). This is supported by the finding that the numbers of thick disc stars in the model are being overestimated (after scaling) because the presence of the CMa structure is boosting the numbers of stars in the region. Although difficult to quantify, it is expected that the numbers of Galactic thick disc stars should be much fewer than the ∼15 stars as currently predicted. Investigation of any similarities to previous detections of the Monoceros Ring finds encouraging agreement in the velocity dispersion estimates of Yanny et al. (2004) and Crane et al. (2003), which have values of 13–24 and $20 \pm 4\,\mathrm{km\,s^{-1}}$, respectively, compared to $22.7 \pm 1.7\,\mathrm{km\,s^{-1}}$ from this paper.

The best model of the Monoceros Ring with which to compare our detection is the Crane et al. (2003) circular orbit model, since we target similar stars (M-giant stars extracted from 2MASS) and since they reach a Galactic longitude of $l \sim 220^\circ$ in the Southern hemisphere and $l \sim 240^\circ$ in the Northern hemisphere. Moreover, as has already been noticed, the velocity dispersion of our sample ($\sigma = 22.7 \pm 1.7\,\mathrm{km\,s^{-1}}$) is statistically similar to the Crane et al.

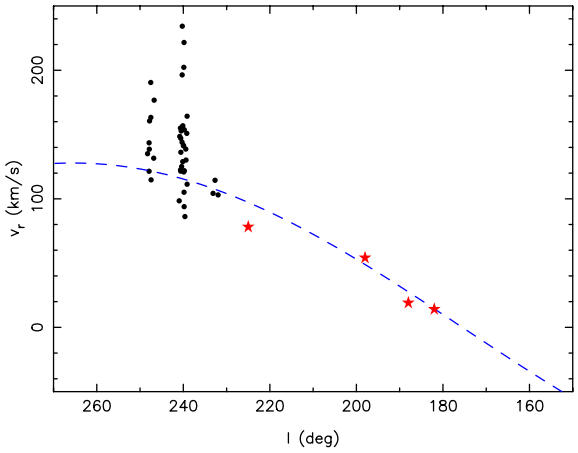

Figure 3. Distribution of the target M-giant stars compared with previous detections of the Monoceros Ring. Stars from our sample are shown as filled circles, whereas SDSS detections are plotted as stars. The dashed line corresponds to the best circular orbit model from Crane et al. (2003) for a population orbiting the Milky Way at $D_{\mathrm{GC}} = 18$ kpc with a rotational velocity of $v_{\mathrm{rot}} = 220\,\mathrm{km\,s^{-1}}$.

value ($20 \pm 4\,\mathrm{km\,s^{-1}}$). It can be seen in Fig. 3, where our targets are plotted as filled circles, that the velocity of our sample is only slightly higher than that expected by the circular model. Such a small discrepancy is not unexpected, since the Monoceros Ring population certainly does not follow a perfectly circular orbit (as is hinted by detections at different Galactocentric distances within the $14 < D_{\mathrm{GC}} < 20$ kpc distance range). Moreover, a closer look at fig. 2 of Crane et al. (2003) reveals that the stars at high longitude

in their sample ($l > \sim 220^\circ$) also tend to have a radial velocity 20–30 km s^{-1} higher than the circular orbit model. Thus our detection of the Monoceros Ring is consistent with the current knowledge of this outer disc structure.

Equatorial accretion models predict the presence of wrapped tidal arms, and this detection provides a tentative confirmation of such a scenario. A plausible alternative is that both the foreground Canis Major detection and the background Monoceros Ring detection represent separate accretion events. However, such a situation complicates the picture with the requirement of two progenitor systems hidden somewhere in the Milky Way. Hence we conclude that the probable scenario is that the Canis Major dwarf and the Monoceros Ring represent a single accretion event and this new detection is of a wrapped tidal arm.

ACKNOWLEDGMENTS

BCC's thanks go to the Anglo-Australian Observatory and the ANU Lodge for the technical support and hospitality received during his stay. GFL acknowledges the support of the Discovery Project grant DP0343508. NFM acknowledges support from a Marie Curie Early Stage Research Training Fellowship under contract MEST-CT-2004-504604.

REFERENCES

Abadi M. G., Navarro J. F., Steinmetz M., Eke V. R., 2003a, ApJ, 591, 499
Abadi M. G., Navarro J. F., Steinmetz M., Eke V. R., 2003b, ApJ, 597, 21
Bellazzini M., Ibata R., Monaco L., Martin N., Irwin M. J., Lewis G. F., 2004, MNRAS, 354, 1263
Bonifacio P., Monai S., Beers T. C., 2000, AJ, 120, 2065
Conn B. C., Lewis G. F., Irwin M. J., Ibata R. A., Irwin J. M., Ferguson A. M. N., Tanvir N. R., 2005, MNRAS, 362, 475
Crane J. D., Majewski S. R., Rocha-Pinto H. J., Frinchaboy P. M., Skrutskie M. F., Law D. R., 2003, ApJ, 594, L119
Ibata R. A., Gilmore G., Irwin M. J., 1994, Nat, 370, 194
Ibata R. A., Irwin M. J., Lewis G. F., Ferguson A. M. N., Tanvir N., 2003, MNRAS, 340, L21
Majewski S. R., Skrutskie M. F., Weinberg M. D., Ostheimer J. C., 2003, ApJ, 599, 1082
Majewski S. R., Ostheimer J. C., Rocha-Pinto H. J., Patterson R. J., Guhathakurta P., Reitzel D., 2004, ApJ, 615, 738
Martin N. F., Ibata R. A., Bellazzini M., Irwin M. J., Lewis G. F., Dehnen W., 2004a, MNRAS, 348, 12
Martin N. F., Ibata R. A., Conn B. C., Lewis G. F., Bellazzini M., Irwin M. J., McConnachie A. W., 2004b, MNRAS, 355, L33
Martin N. F., Ibata R. A., Conn B. C., Lewis G. F., Bellazzini M., Irwin M. J., 2005a, MNRAS, 362, 906 (Paper I)
Martin N. F., Ibata R. A., Conn B. C., Irwin M. J., Lewis G. F. 2005b, Publ. Astron. Soc. Aust., 22, 236
Martínez-Delgado D., Peñarrubia J., Dinescu D. I., Butler D. J., Rix H. W., 2005, preprint (astro-ph/0506012)
Newberg H. J. et al., 2002, ApJ, 569, 245
Peñarrubia J. et al., 2005, ApJ, 626, 128
Press W. H., Teukolsky S. A., Vetterling W. T., Flannery B. P., 1992, Numerical Recipes in FORTRAN: The Art of Scientific Computing 2nd edn. Cambridge Univ. Press, Cambridge
Robin A. C., Reylé C., Derrière S., Picaud S., 2003, A&A, 409, 523
Rocha-Pinto H. J., Majewski S. R., Skrutskie M. F., Crane J. D., 2003, ApJ, 594, L115
Rocha-Pinto H. J., Majewski S. R., Skrutskie M. F., Crane J. D., Patterson R. J., 2004, ApJ, 615, 732
Schlegel D. J., Finkbeiner D. P., Davis M., 1998, ApJ, 500, 525
Searle L., Zinn R., 1978, ApJ, 225, 357
Taylor K., Bailey J., Wilkins T., Shortridge K., Glazebrook K., 1996, in Jacoby G. H., Barnes J., eds, ASP Conf. Ser. Vol. 101, Astronomical Data Analysis Software and Systems V. Astron. Soc. Pac., San Francisco, p. 195
White S. D. M., 1978, MNRAS, 184, 185
White S. D. M., Rees M. J., 1978, MNRAS, 183, 341
Yanny B. et al., 2004, ApJ, 605, 575

This paper has been typeset from a TEX/LATEX file prepared by the author.